Astron. Astrophys. 338, 947–956 (1998)

ASTRONOMY
AND
ASTROPHYSICS

Phase-resolved optical photometry and spectroscopy of the supersoft X-ray binary 1E 0035.4-7230⋆

A. van Teeseling[1], **K. Reinsch**[1], **M.W. Pakull**[2], **and K. Beuermann**[1]

[1] Universitäts-Sternwarte Göttingen, Geismarlandstrasse 11, D-37083 Göttingen, Germany
[2] Observatoire de Strasbourg, URA 1280 du CNRS, F-6700 Strasbourg, France

Received 7 May 1998 / Accepted 3 August 1998

Abstract. We present phase-resolved optical photometry and spectroscopy of the supersoft X-ray binary 1E 0035.4-7230 (= SMC 13). The average U, B, V, and R light curves show an almost perfect sinusoidal $\Delta m \sim 0.3$ mag modulation on the 4.1 hr orbital period, but in individual binary orbits there can be significant deviations from the average light curves. There is a significant $B-V$ variability with a standard deviation of 0.04 mag, and which may be related to the orbital phase. The binary appears to be bluest $\sim 0.2-0.3$ in orbital phase before optical minimum. Modeling of the light curves indicates an orbital inclination of $\sim 20-50^\circ$ and a mass ratio $M_1/M_2 < 3$ (with M_1 the mass of the accreting star). The observed optical modulation is probably dominated by the changing aspect of the irradiated companion star, which has effective temperatures on the irradiated side $\gtrsim 30\,000$ K. Our spectra show variable He II$\lambda 4686$ emission, and broad Balmer absorption lines. The latter appear more prominent when the companion star is closest to us. Modeling the optical spectrum of the irradiated companion star by a composition of normal stellar spectra reproduces the observed colour and amplitude of the modulation, but predicts too strong Balmer absorption lines which must be significantly weaker because of strong irradiation.

Key words: accretion, accretion disks – stars: individual: 1E 0035.4-7230 – novae, cataclysmic variables – white dwarfs – X-rays: stars

1. Introduction

Supersoft X-ray binaries are accreting binaries which are observationally distinguished by very soft X-ray spectra with almost all flux below 0.5 keV and luminosities close to the Eddington luminosity of a solar mass star (see reviews by Kahabka & Van den Heuvel 1997; Van Teeseling 1998). Most of the known supersoft X-ray binaries are located in the Magellanic Clouds. In the galactic disk, the high interstellar absorption limits the distance of detectable supersoft X-ray binaries to ~ 2 kpc. Although a few classical and symbiotic novae (Ögelman et al. 1993; Jordan et al. 1994) appeared as a supersoft X-ray source after a nova outburst, most supersoft X-ray binaries have optical properties reminiscent of those of low-mass X-ray binaries (see overview by Van Teeseling 1998). This suggests that their optical and ultraviolet spectra are strongly affected by soft X-ray irradiation from the accreting compact star.

ROSAT, BEPPOSAX, and ASCA X-ray spectra of most supersoft X-ray binaries are consistent with that of a very hot white dwarf (Van Teeseling et al. 1996a; Parmar et al. 1998; Ebisawa et al., in prep.). Van den Heuvel et al. (1992) argued that the observable properties of supersoft X-ray binaries like CAL 83 and CAL 87 can be explained with stable steady-state shell burning of the accreted hydrogen on a massive white dwarf. In systems which do not have a sufficiently high accretion rate for steady-state shell burning, the accreted hydrogen burns recurrently during which the binary also may appear as a supersoft X-ray source (Iben 1982; Fujimoto 1982). The necessary high accretion rate for stable steady-state or recurrent hydrogen shell burning could be obtained with thermal-timescale mass transfer from a $\sim 1.3-2.5 M_\odot$ near-main-sequence star (Van den Heuvel et al. 1992). Alternatively, the high mass transfer may be the result of the nuclear shell burning itself and be driven by strong mass loss from a strongly irradiated low-mass donor star (Van Teeseling & King 1998).

1E 0035.4-7230 (hereafter 1E 0035) was discovered with EINSTEIN as a very soft X-ray source in the direction of the Small Magellanic Cloud (Seward & Mitchell 1981). ROSAT observations revealed a supersoft X-ray spectrum with a blackbody temperature of ~ 40 eV (Kahabka et al. 1994). If 1E 0035 is located in the SMC, its bolometric luminosity is $\sim 10^{37}$ erg s^{-1} (Van Teeseling et al. 1996a). Orio et al. (1994) have identified 1E 0035 with a $B \sim 20$ variable blue star. Schmidtke et al. (1996; hereafter S96) have shown that this optical counterpart undergoes nearly sinusoidal variations with a period of 4.13 hr and a peak-to-peak amplitude of $\Delta V \sim 0.3$ mag. 1E 0035 is particularly interesting among the supersoft X-ray binaries, because its short orbital period excludes the scenario in which the shell burning on the white dwarf is powered by thermal-timescale mass transfer from a more massive companion star. Kahabka & Ergma (1997) have therefore proposed that 1E 0035 is a cataclysmic variable, currently in a phase of residual hydrogen burning after a mild shell flash. However, as suggested by

⋆ Based on observations collected at the European Southern Observatory, La Silla, Chile: ESO N° 56.D-0589, 58.D-0275

Van Teeseling & King (1998), 1E 0035 may be doomed to remain a supersoft X-ray binary for millions of years if the mass transfer has been raised sufficiently by the strong soft X-ray irradiation of the companion star. In the course of its evolution, its orbital period would increase and turn 1E 0035 into a system resembling the long-period supersoft X-ray binaries.

In this paper we present phase-resolved optical photometry and spectroscopy of 1E 0035. We constrain the binary parameters by modeling the photometric light curve and focus on the observational effects of the very strong irradiation of the companion star. We also compare our results with those of Crampton et al. (1997; hereafter C97).

2. Observations

2.1. Photometry

We obtained CCD photometry of 1E 0035 in U, B, V, and R with EFOSC-2 at the ESO/MPI 2.2m telescope at La Silla. The images were obtained over three subsequent nights in December 1996 (JD 2 450 434.56 – 2 450 436.72) under photometric conditions with a seeing varying between 1.0″ and 1.3″. Each night, we observed the source over roughly one complete binary orbit with series of BVR, UBV, or $UBVR$ sequences. This resulted in 25 U images, 37 B images, 38 V images, and 24 R images. Relative fluxes were obtained by integrating the measured intensities within apertures centered on the star and with $1.05''$ radii (4 pixels). With 5 min U and B exposures and 4 min V and R exposures, typical errors in the derived differential magnitudes are 0.04 mag in U and 0.02 mag in B, V, and R. Mean magnitudes in the Johnson-Kron-Cousins photometric system were estimated by comparison with Landolt standard stars (Landolt 1992) observed at the beginning and end of the night. During our photometry run, the mean magnitudes of 1E 0035 were $V = 20.3$, $U - B = -1.3$, $B - V = -0.1$, and $V - R = 0.0$.

2.2. Spectroscopy

In October 1995 (JD 2 450 005.51 – 2 450 007.66), we obtained 12 spectra of 1E 0035 with EFOSC-1 at the 3.6m telescope at La Silla. Each spectrum has an exposure of 30 min and covers the wavelength range of 3750–6950 Å. Most exposures were obtained during photometric conditions with a seeing of $\sim 1.5''$. With a spectral dispersion of ~ 6 Å/pixel and a 1.5″ slit, the resulting FWHM resolution was ~ 15 Å. We minimized the loss of light due to differential atmospheric refraction by rotating the slit before each exposure to make it perpendicular to the horizon. To obtain an accurate wavelength calibration, each exposure was followed by a He-lamp observation with the telescope pointed to the same direction. The spectra have been flux calibrated using the standard stars LTT 7987 and LTT 2415 (Stone & Baldwin 1983).

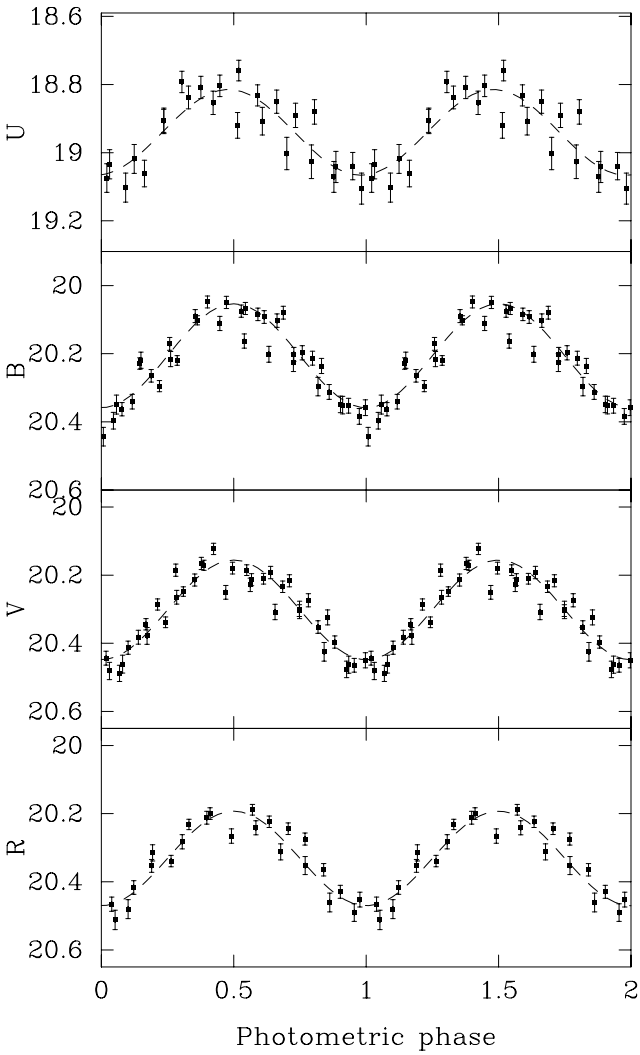

Fig. 1. U, B, V, and R light curves of 1E 0035 folded on the orbital ephemeris. The dashed lines are χ^2 fits of the data to sine curves, with best-fit parameters given in Table 1

3. Results from photometry

3.1. Orbital period and light curve

In all four colour bands, the light curve shows the almost perfectly sinusoidal modulation reported by S96 and C97. We did not perform a systematic period search, but determined the minima in each light curve by fitting a sine curve. Combining our B, V, and R photometric minima with the time of minimum light given by C97 gives an orbital ephemeris of

$$T_0 = \mathrm{HJD}\,2\,450\,434.1320(6) + 0.1719260(7)E \qquad (1)$$

where T_0 defines the time of minimum optical light. Our orbital period is consistent with those given by S96 and C97. (Note that the 0.172007-day alias period found by C97 results in a phase offset of 10% of the orbital period.) In the remaining part of this paper we will use the above ephemeris.

Fig. 1 shows the phase-folded light curves in the four colour bands. We have fitted each phase-folded light curve with a sine

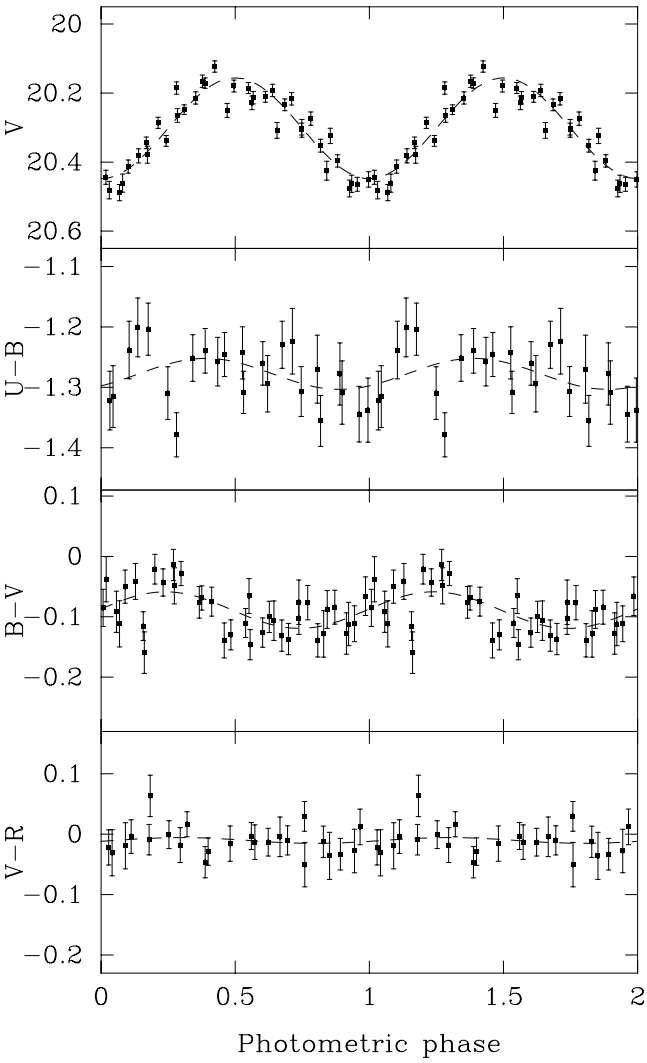

Fig. 2. V, $U-B$, $B-V$, and $V-R$ light curves of 1E 0035 folded on the orbital ephemeris. The dashed lines are χ^2 fits of the data to sine curves, with best-fit parameters given in Table 1

Table 1. Parameters of a sine fit $m = C + A\sin[2\pi(\phi + 0.25 - \phi_0)]$ to phase-folded U, B, V, and R light curves of 1E 0035. ϕ_0 is the phase of minimum light or maximum redness; 1σ errors of the last digit(s) are given in parentheses

band	C	A	ϕ_0
U	18.9	0.13(1)	0.98(2)
B	20.2	0.150(4)	0.00(1)
V	20.3	0.144(4)	0.00(1)
R	20.3	0.137(7)	0.00(2)

colour	C	A	ϕ_0
$U-B$	−1.3	0.026(13)	0.89(6)
$B-V$	−0.1	0.030(7)	0.74(4)
$V-R$	0.0	0.005(8)	–

curve, leaving the amplitude, phase and offset of the sine free. The best-fit sine parameters (see Table 1) show that, within the uncertainties, the amplitude of the modulation is the same in all colour bands. In Fig. 2, we have plotted the phase-folded $U-B$, $B-V$, and $V-R$ light curves, where we have only combined data obtained immediately after each other. Only $B-V$ is significantly variable ($P = 0.3\%$) with a standard deviation of 0.04 mag. Since the $B-V$ variability is also significant within a single binary orbit, it is probably the result of a true orbital modulation and not of orbit-to-orbit light curve changes. The amplitude of the best-fit sinusoidal modulation is 0.03 mag in $B-V$, with possibly a similar modulation in $U-B$. Surprising is that the $B-V$ modulation (and perhaps also the $U-B$ modulation) shows a large phase shift with respect to the V modulation: the binary appears bluest at photometric phase ~ 0.8. The phasing of the $U-B$ and $B-V$ modulation suggests that the colour modulation may be related to the accretion stream-disk interaction (our light curve modeling in Sect. 3.2 suggests that we observe the 'bright spot' on the accretion disk rim face-on at phase ~ 0.8). However, given the almost perfect sinusoidal shape of the light curves, any effect of such an accretion-disk bright spot on the light curves is apparently small. The small amplitude of the colour light curves implies that the difference in flux between maximum and minimum orbital light has roughly the same colours and spectrum as the mean spectrum of 1E 0035. We will investigate this in more detail in Sect. 5.

In addition to the orbital sinusoidal modulation, the optical light curve of 1E 0035 shows a large amount of cycle-to-cycle variability. As shown in Fig. 3, within one binary orbit the light curve can be almost perfectly sinusoidal, while showing pronounced deviations from a sinusoid during other binary cycles. Such cycle-to-cycle variability has also been observed in other supersoft X-ray binaries (e.g. Smale et al. 1988; Meyer-Hofmeister et al. 1998). We do not find, however, any evidence for an asymmetric minimum as claimed by C97. To test the significance of a possible asymmetry, we have calculated the mean V magnitude in the phase intervals 0.75–0.95 and 0.05–0.25, both for our data and for the data tabulated by C97 folded with our ephemeris Eq. 1. With the data of C97, we find a significant difference of 0.078 ± 0.009 mag between ingress and egress. However, when we fit a sine curve to the V data of C97 folded on the ephemeris given in Eq. 1, we find a phase offset of 0.03, which disappears using a slightly longer period of ~ 0.1719275 days. Using this longer period, the difference in ingress and egress in the folded V data of C97 reduces to 0.035 ± 0.009 mag. This suggests that the asymmetry in the data of C97 may be at least partly the result of the uncertainty in the time of minimum light. With our data the difference is only 0.007 ± 0.011 mag. In any case, the asymmetry, if real, is not persistent, which is confirmed by the large cycle-to-cycle deviations in both data sets.

3.2. Modeling of the light curves

3.2.1. The binary light curve code

To model the photometric light curves, we have written a light-curve code called BINARY++ which calculates the phase-dependent flux at a particular wavelength of a rotating accreting binary consisting of a Roche-lobe filling donor star, an accretion disk, and an extended accreting star (see e.g. Avni 1978;

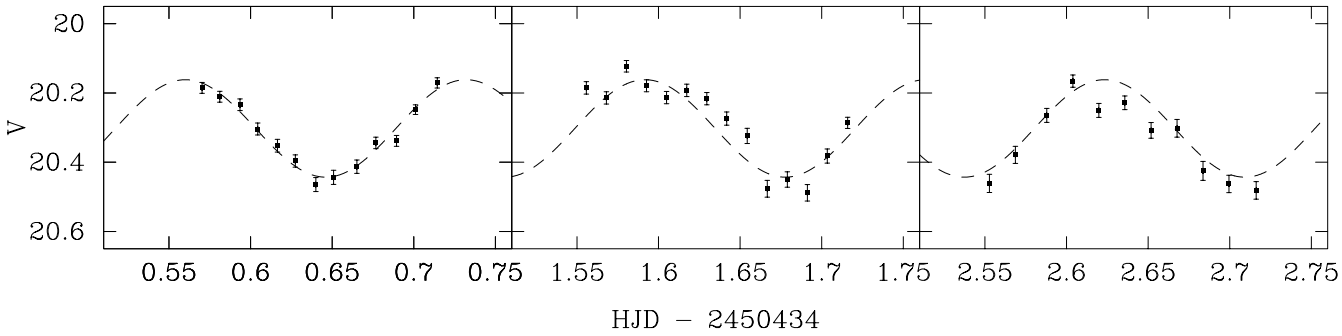

Fig. 3. V light curve of 1E 0035 observed with the 2.2m telescope at La Silla in December 1996. The dashed line is a χ^2 fit of the total data set to a single sine curve (the same as in Fig. 1)

Kopal 1959). We assume that the accreting star is a white dwarf with finite radius, although our results for 1E 0035 are practically the same when we use a point-like X-ray source. Each component, including the accreting white dwarf, is described by a carefully chosen surface grid, where each surface element has its own gravitational potential, area, temperature, coordinate vector, and normal vector. The temperature of the accretion disk is the result from frictional heating according to the optically-thick steady thin disk approximation and from irradiation. The disk has a concave and axisymmetric shape with half thickness proportional to $r^{9/7}$, with r the radial distance from the white dwarf center. The numerical value of the exponent has been derived by assuming that the temperature in the disk is dominated by the reprocessing of irradiation flux (Vrtilek et al. 1990). The accretion disk and the gravity-darkened donor star are irradiated by the luminous accreting star, where the amount of irradiation is calculated by determining the irradiating flux from each white-dwarf surface element. The calculations take into account possible mutual eclipses by the accretion disk and the donor star, shielding of the accretion disk flux by the disk rim (because of the concave shape of the disk), and mutual shielding of the extended accreting white dwarf and the (inner) accretion disk (the disk extends to the white dwarf surface and shields one half of the white dwarf).

The flux from each surface element is calculated using a blackbody approximation. We note that a blackbody approximation gives roughly the correct optical colour for an irradiated atmosphere, but may significantly overestimate the amount of optical flux (Hessman et al. 1997). This has been taken into account by introducing an irradiation parameter $l \equiv 10^{-12}\eta L_{\rm x}/(4\pi a^2)\,[10^{-12}\,{\rm erg\,s^{-1}cm^{-2}}]$, where $L_{\rm x}$ is the white dwarf luminosity, a the orbital separation of the stars, and η a reprocessing efficiency factor. η includes uncertainties like the fraction of irradiating flux which is being reprocessed and the spectrum of the reprocessed radiation. In principle, η depends on the wavelength, on the physical parameters of the irradiated atmosphere, and on the spectrum and incidence angle of the irradiation. In the present calculations, however, we assume a uniform and wavelength-independent value for η (and therefore also for l). The introduction of l makes the calculation of the shape of the light curve independent of the orbital separation a and reduces the amount of fit parameters by using the fact that only the product of η and $L_{\rm x}$ goes into the calculations.

Limb darkening is approximated with a standard linear limb-darkening law. Because there are, to our knowledge, no published limb-darkening coefficients $u(\lambda)$ for irradiated atmospheres, and because the complicated temperature structure in an irradiated atmosphere may reduce limb darkening and even produce limb brightening at certain wavelengths, we use a wavelength-independent limb-darkening coefficient, varying between gray limb darkening with $u = 0.6$ and no limb darkening with $u = 0$.

Schandl et al. (1997) have also calculated light curve models for supersoft X-ray binaries. We emphasize that there are some fundamental differences between our model and that of Schandl et al. and the choice of fit parameters. For the present application to the data of 1E 0035, we do not include an optically thick, radially and azimuthally extended disk rim, which according to Schandl et al. would be the result of a spray originating at the accretion stream-disk interaction. We do not find any evidence (see Sect. 3.1) for an azimuthal asymmetry in our U, B, V, and R light curves of 1E 0035 (although there is some evidence from the $B-V$ data), and can model the light curves successfully (and better) without an additional thick rim. However, we leave the angular thickness of the disk as a free parameter. We only fit the relative light curves (i.e. with an arbitrary magnitude offset) such that the results are independent of the unknown orbital separation a, but use the observed absolute magnitude as a consistency check on the inferred distance. As mentioned above, the white dwarf luminosity and the reprocessing efficiency are combined in the parameter l.

3.2.2. Model parameters used for 1E 0035.4-7230

In Table 2, we summarize the model parameters used. Because the optical flux is completely dominated by reprocessed irradiation, the amplitude of the modulation (but not the absolute magnitude) is relatively insensitive to the value of l. Therefore, we have fixed $l = 100$, corresponding to $\eta L_{\rm x} \approx 10^{37}\,{\rm erg\,s^{-1}}$ and $a \approx 9 \times 10^{10}\,{\rm cm}$. It also turns out that the optical flux is completely dominated by irradiation effects, and that the results do not depend very much on the polar temperature T_2 of

Table 2. Summary of input model parameters used to fit the U, B, V, and R light curves of 1E 0035

parameter	description	value
Q	mass ratio M_1/M_2	free
i	orbital inclination	free
f	outer radius of disk/Roche-lobe radius	free
β	angular half-thickness of disk	free
μ	linear limb-darkening coefficient	$0-0.6$
l	$10^{-12}\eta L_{\rm x}/(4\pi a^2)$	100
T_2	polar temperature of secondary	3 000 K
$T_\star$	viscous temperature of disk[a]	125 kK
R_1	white dwarf radius, inner radius of disk	$0.01a$

[a] $T_\star \equiv \left(\frac{3GM_1\dot{M}}{8\pi R_1^3\sigma}\right)^{1/4}$

the donor star (for $T_2 \lesssim 5\,000$ K) or on the viscous temperatures in the accretion disk. We have therefore fixed $T_2 = 3\,000$ K and $T_\star = 125\,000$ K.

Assuming a main-sequence donor star, the orbital period of 1E 0035 implies a donor star mass of $M_2 \sim 0.4M_\odot$. If the donor star has expanded and has a lower density than a main-sequence star, its mass must be $M_2 < 0.4M_\odot$. An orbital period of 4.13 hr also implies an orbital separation of $(0.8-1.1)\times10^{11}$ cm: e.g. an accreting compact star with mass $M_1 = 0.7M_\odot$ ($1.4M_\odot$) gives an orbital separation of $\sim 0.9\times10^{11}$ cm ($\lesssim 1.1\times10^{11}$ cm), almost independent of the donor star mass. A primary with $M_1 \gtrsim 0.7M_\odot$ (necessary to have stable hydrogen shell burning on a white dwarf) and a donor star with $M_2 < 0.4M_\odot$ limits the possible mass ratio to $Q = M_1/M_2 \gtrsim 1.7$.

For all fits, we have fixed the white dwarf radius to $0.01a$, which is consistent with LTE white dwarf fits to the ROSAT spectrum of 1E 0035 (Van Teeseling et al. 1996a). The remaining free fit parameters are the mass ratio $Q = M_1/M_2$, the angular half-thickness β of the disk, the outer disk radius as fraction f compared to the effective Roche-lobe radius according to Eggleton's (1983) approximation, and the orbital inclination i.

3.2.3. Results of χ^2 fits with light curve models

Using χ^2 fits, the best-fit light curve was determined for each set of fixed parameters. The shape of the light curves is best fit with a very small or very flat disk, such that the light curve is essentially that of the rotating irradiated donor star. However, because the binary is much fainter without an irradiated disk, 1E 0035 would be located somewhere halfway to the SMC if it has a very small or flat disk, unless we assume a much higher $\eta L_{\rm x}$ which would not be consistent with the X-ray spectrum. To reproduce absolute magnitudes appropriate for an SMC distance, we have therefore also fixed the disk radius to 80% of the effective Roche-lobe radius, and assumed a non-zero angular half-thickness of the disk. For all parameter choices, no limb darkening produces a slightly better fit than with limb darkening. No limb darkening would be consistent with a temperature gradient in the accretion disk and donor star atmospheres which is flattened by irradiation. However, our results do not exclude other limb-darkening values.

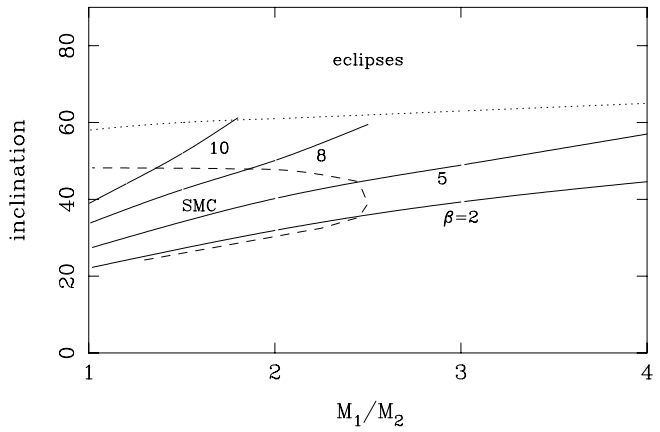

Fig. 4. Orbital inclination of 1E 0035 as function of the mass ratio M_1/M_2 for different values of the angular half-thickness β of the accretion disk (solid lines). The other input model parameters are given in Table 2. Above the dotted line, the model light curves show eclipses which deviate significantly from the observed light curves. A location in the SMC, limits the possible solutions to those to the left of the dashed curve, which corresponds to a distance of 50 kpc and a visual extinction of $A_{\rm V} \approx 0.2$ (see text)

The inferred inclination as a function of β and Q is shown in Fig. 4. With increasing β, the accretion disk becomes brighter, the heating of the companion star less, and the inferred inclination higher. However, if the inclination is higher than $\gtrsim 65^\circ$ (somewhat depending on Q), the donor star eclipses part of the disk and vice versa, and the light curves show eclipses which deviate significantly from the observed light curve. Assuming $Q > 1.5$, this limits the possible angular half-thickness of the disk to $\beta \lesssim 10^\circ$.

The SMC is known to have a significant depth of ~ 20 kpc with a mean distance of ~ 60 kpc (see Westerlund 1997 and references therein). It is likely, however, that 1E 0035 is located on the near side of the SMC, because else it would show a larger amount of absorption in the soft X-ray band. A distance of at least 50 kpc (distance modulus $\gtrsim 18.5$ mag) and a reddening of $E_{\rm B-V} \sim 0.06$ limits the possible mass ratio (using $a \approx 10^{11}$ cm) to $Q \lesssim 2.5$ and the inclination to $i \lesssim 50^\circ$ (systems with $Q > 2.5$ or $i > 50^\circ$ would be fainter than observed at a distance > 50 kpc). If we also assume a companion star with a density of a main-sequence star or less, and a mass of the accreting star $> 0.6M_\odot$ (see Sect. 3.2.2), the inferred mass ratio is in the range of $M_1/M_2 \sim 1.5-2.5$. However, without constraints on the distance and absolute magnitude of the system and on the masses of both stars, lower or higher mass ratios cannot be excluded. With a main-sequence companion star, a mass ratio $Q < 2.5$ corresponds to a mass of the accreting star of $< 1M_\odot$. It is possible to relax the upper limit on the mass ratio and inclination by assuming a higher irradiation parameter l (see Fig. 4).

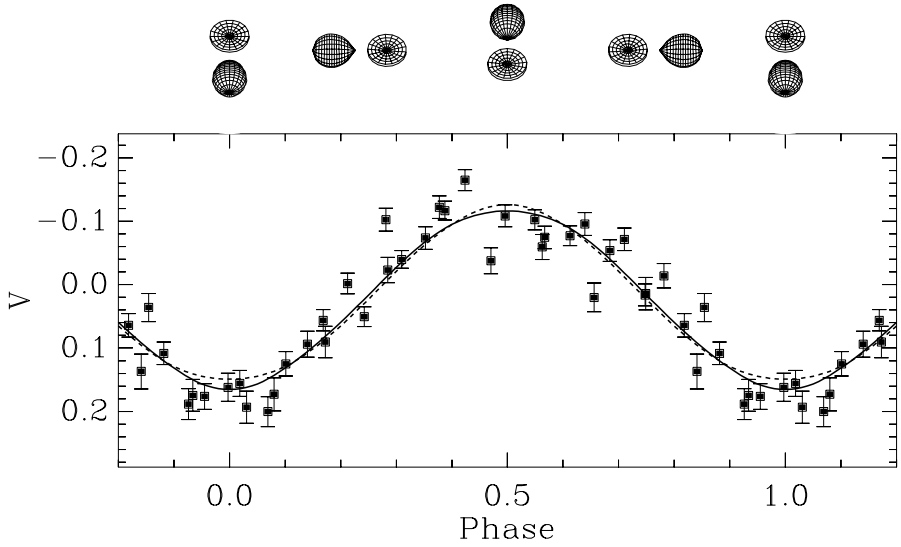

Fig. 5. Phase-folded V light curve of 1E 0035 together with best-fit model light curves for $Q = 2$ (solid line) and $Q = 4$ (dashed line). The accretion disk radius is fixed to $f = 0.8$ and its angular half-thickness to $\beta = 5°$. The binary plotted above the frame corresponds to the $Q = 2$ light curve with best-fit inclination of $i = 40°$

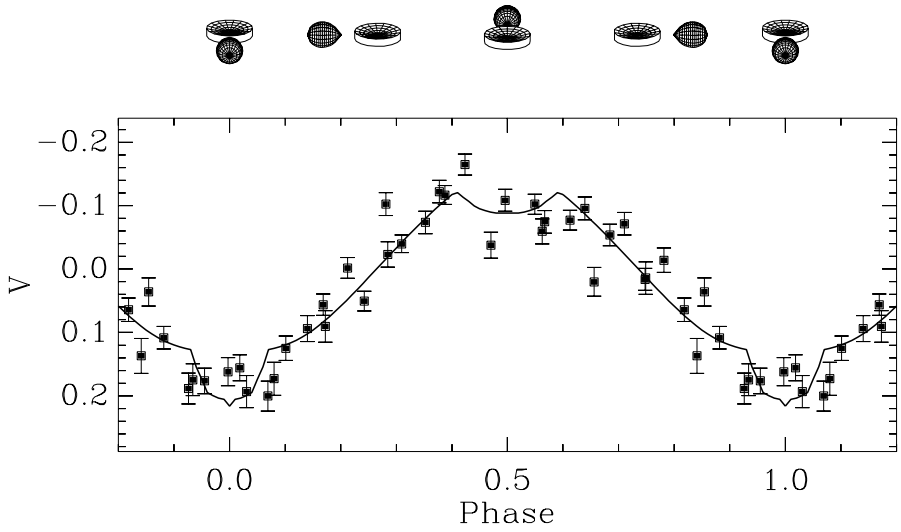

Fig. 6. Same as Fig. 5, but with best-fit model light curve for $Q = 5$, and with the inclination and irradiation fixed to $i = 70°$ and $l = 200$, respectively. The best-fit angular half-thickness of the disk is $\beta = 9.6°$

Fig. 5 shows the observed phase-folded V light curve together with the fitted light curves for no limb darkening, $\beta = 5°$, and mass ratio's $M_1/M_2 = 2$ and 4. Minimum optical light corresponds to inferior conjunction of the companion star. Our model light curves are consistent with the light curves observed by C97, especially when we use a slightly longer period as discussed in Sect. 3.1. Fitting the data of C97 gave very similar results, but did (because of the larger errors of the data points) not lead to stronger constraints on the fit parameters.

We note that the light curve models do not fit the observed light curves much better than a simple sine curve, which illustrates the almost perfectly sinusoidal shape of the light curves: our analysis shows that the optical modulation is probably completely the result of the changing aspect of the irradiated donor star and that an eclipse of the accretion disk by the companion star, such as suggested by C97, is not the major (and probably also not a minor) cause of the light curve minimum. Our model suggests a moderate inclination of $i \sim 20° - 50°$. An inclination $> 70°$ would not only produce a deeper and narrower minimum, but also place 1E 0035 closer than the SMC. We cannot exclude, however, a shallow eclipse, provided that the amount of irradiation is significantly larger than estimated above: e.g. with a fixed inclination of $\sim 70°$ and $l = 200$, it is possible, as shown in Fig. 6, to get a reasonable fit and a distance ~ 50 kpc with $Q = 5$ and $\beta \approx 10°$. Such a high value of l, however, implies a rather high luminosity of the accreting star and reprocessing efficiency. The conclusion of C97 that the inclination is likely to lie in the range $\sim 70° - \sim 78°$ is mainly based on an asymmetrical minimum, which at least in our data does not exist (see Sect. 3.1). The fact that the light curve modulation is entirely the result of the changing aspect of the irradiation-heated secondary does not, as C97 argue, imply that we might expect to see spectral signatures from this star, since the spectrum of a strongly irradiated atmosphere may be completely different of that of an unirradiated atmosphere (see Sect. 5).

Since the optical flux is dominated by reprocessed soft X-rays, and the inclination is probably not very high, the observed

optical cycle-to-cycle and long-term variability may reflect the X-ray variability of 1E 0035 or a variable amount of irradiation e.g. because of a variable angular thickness of the disk.

4. Results from spectroscopy

Some preliminary results of our spectroscopy have been presented by Van Teeseling et al. (1996b). Although our spectra have a much lower spectral resolution than those of C97, we will discuss them again in some more detail in the context of our photometric results, and because they appear to be significantly different, with more prominent Balmer absorption, than those presented by C97.

4.1. Average spectrum

The average spectrum is shown in Fig. 7. Using only the spectra obtained during the photometric first two nights, we derive an average magnitude of $V = 20.4$ and a $B - V$ colour of ~ -0.1, which are consistent with the values derived from our photometry.

The average spectrum shows clear He IIλ4686 emission with an equivalent width of ~ 2 Å and a radial velocity of $\sim +500\,\mathrm{km\,s^{-1}}$. It is possible that there is also very weak He IIλ5412 and O VIλ5291 emission. Hβ is in absorption with an average equivalent width of ~ 2 Å and a radial velocity of $\sim +300\,\mathrm{km\,s^{-1}}$. In the average spectrum there is no clear evidence for Balmer absorption lines other than Hβ. The He IIλ4686 emission and the Hβ absorption are consistent with the spectra obtained by S96 and C97, except for the much higher mean radial velocities.

The FWHM of the normalized average He IIλ4686 is ~ 18 Å, which is comparable to the spectral resolution. The FWHM of the normalized average Hβ is ~ 22 Å. The phase-resolved spectra and the results of C97 show that this non-zero intrinsic width of Hβ is the result of a variable radial velocity and of a significant intrinsic broadening in some spectra.

We do not find any evidence for Hα emission as observed by C97. Since the equivalent width of the Hα+He II blend in the spectra of C97 is significantly larger than that of He IIλ4686, we would have detected similar Hα emission, even with our much lower spectral resolution. Clearly, the phase-averaged optical spectrum of 1E 0035 is variable, which may be the result of a variable amount of irradiation. Indeed, C97 mention that 1E 0035 was somewhat brighter during their spectroscopic run, than during earlier observations.

4.2. Phase-resolved spectra

The average flux level of the 4 spectra in the phase interval from -0.12 to 0.13 ($\langle|\phi|\rangle = 0.09$) is lower by about $\Delta V \sim 0.1$ than that of the 5 spectra in the phase interval from 0.25 to 0.43 ($\langle\phi\rangle = 0.34$), which is consistent with the photometric orbital modulation. For both averaged spectra we find $B - V \sim -0.1$.

Although Hβ is the only clear absorption feature in the average spectrum, some of the spectra, as shown in Fig. 8, also show

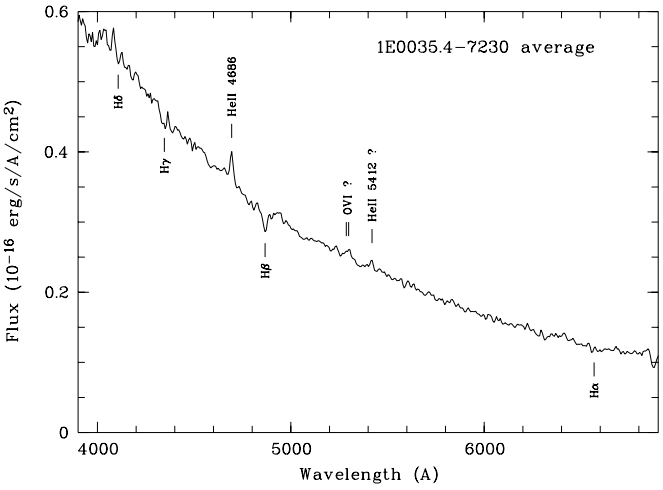

Fig. 7. Average flux-calibrated spectrum of 1E 0035

other Balmer lines (including Hα) in absorption. The Balmer absorption lines seem to be more prominent near optical orbital minimum, i.e. when the companion star is closest to us. Also C97 found that Hγ absorption appeared to be strongest near minimum light.

To increase the signal-to-noise ratio, we have combined the three spectra taken in the first night (with phases 0.05, 0.29, and 0.46) with the first three spectra taken in the second night (with phases 0.10, 0.28, and 0.46). We have normalized each spectrum by fitting a spline function to the continuum and dividing the spectrum by this spline. Fig. 9 shows all normalized spectra and the normalized average spectrum in the wavelength region containing He IIλ4686 and Hβ: both the He IIλ4686 emission and the Hβ absorption are variable in strength and wavelength.

We have measured the radial velocity of He IIλ4686 and Hβ in each of the 9 normalized spectra by cross-correlating the spectra with the normalized average spectrum *and* by fitting Gaussian profiles to the lines. The He IIλ4686 radial velocity shows a large 1σ variability of $\sim 180\,\mathrm{km\,s^{-1}}$, but we could not correlate this variability with the photometric orbital phase. The Hβ radial velocity, however, shows a 99% significant correlation with the photometric orbital phase, and has the blue-to-red zero crossing close to minimum optical light (Van Teeseling et al. 1996b). Better spectra are required to confirm the reality of this correlation between the Hβ radial velocity and the orbital phase. The semi-amplitude of a sine fit to the Hβ radial velocity is $\sim 150\,\mathrm{km\,s^{-1}}$. The average radial velocity of Hβ, corrected for the earth's motion, is $\sim +300\,\mathrm{km\,s^{-1}}$. This is significantly higher than the mean heliocentric radial velocity of the SMC of $\sim +150\,\mathrm{km\,s^{-1}}$ (with a spread of $\sim 50\,\mathrm{km\,s^{-1}}$; see Westerlund 1997 and references therein) and the mean Hα (emission) velocity of $-88\,\mathrm{km\,s^{-1}}$ measured by C97.

5. The spectrum of the companion star and the origin of the Balmer lines

The possible correlation of the Hβ radial velocity with the photometric orbital phase suggests that part of the Hβ absorption

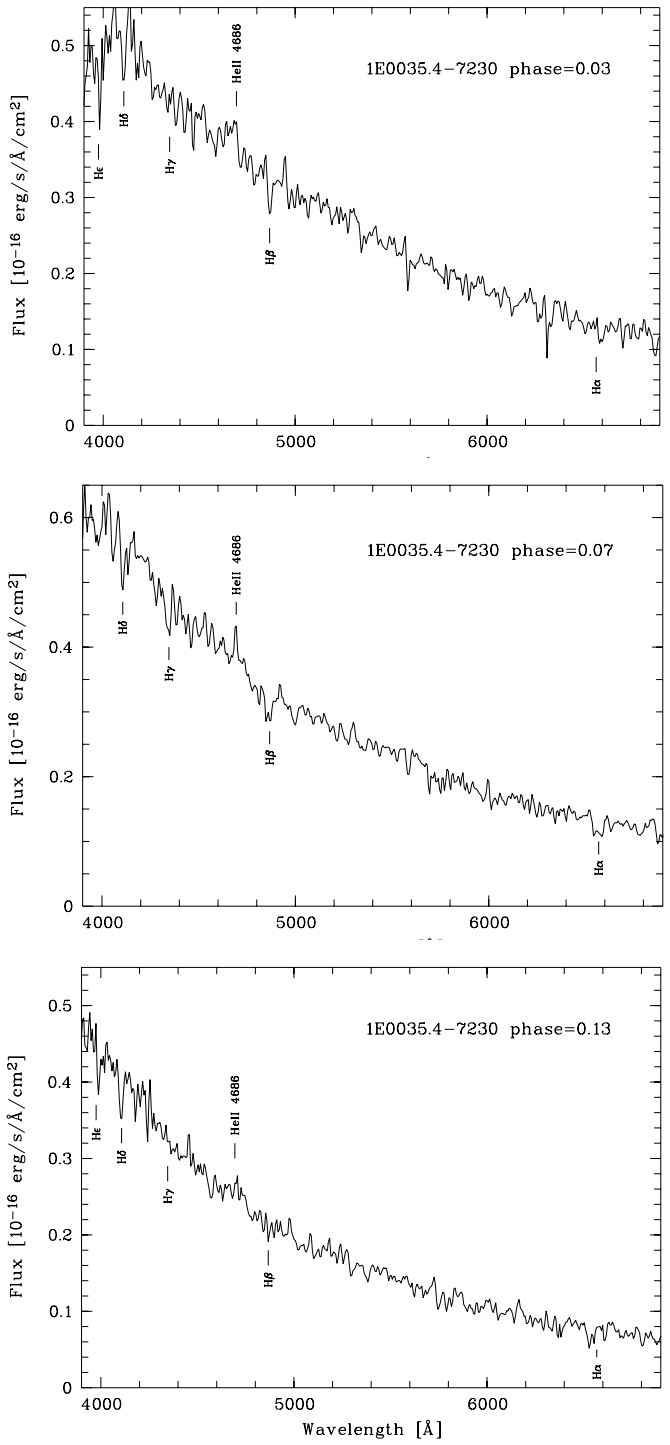

Fig. 8. Flux-calibrated spectra of 1E 0035 near optical minimum

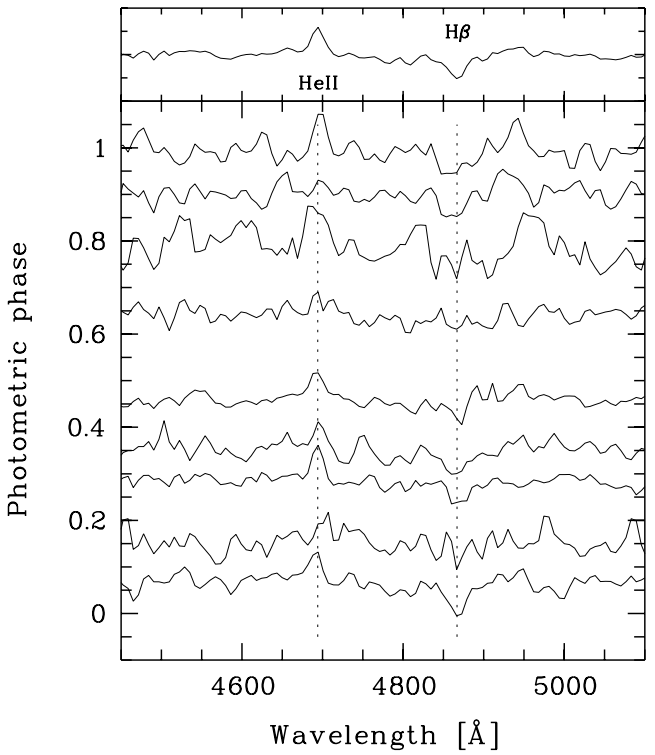

Fig. 9. Normalized spectra at different photometric phases. The top panel shows the normalized average spectrum. The dotted lines give the average wavelengths of the He IIλ4686 emission and the Hβ absorption

traces the orbital motion of the companion star. However, given the low signal-to-noise ratio and spectral resolution of our spectra, we cannot make a firm statement on the origin of the Balmer absorption. The large FWHM of Hβ in some spectra suggests that the Hβ absorption is contaminated with a variable broad absorption component of a different origin. This broad absorption may be double-peaked or contaminated with an emission core as observed by C97.

From our light curve modeling in Sect. 3, we find that the maximum effective temperature of the irradiated surface of the companion star may exceed 30 000 K (if there is not some kind of very effective heat transport from the irradiated side to the unirradiated side). The mean effective temperature of the heated side is that of an O or B star, while the intrinsic effective temperature of the companion, and that of the unirradiated side, is only that of an (unobservable) M star.

As a first approach to model the spectrum of the irradiated companion star, we have composed artificial spectra by using observed stellar spectra (Jacoby et al. 1984). We have taken the temperature distribution of the companion star from our best-fit light curve solution with $Q = 2$ and $\beta = 5°$. Then, we have assigned observed stellar spectra with the appropriate effective temperature and flux to each projected surface element, and summed the flux of all visible surface elements. In Fig. 10, we have plotted the observed phase-averaged spectrum of 1E 0035 scaled to $V = 20.3$, and the artificial spectra for orbital phases 0 and 0.5. The artificial spectra have been convolved with a Gaussian of 15 Å FWHM, and have the same spectral resolution as the observed spectrum. The artificial spectrum of the companion star resembles that of a B star both at orbital minimum and maximum. The colours of the spectra of the companion star are roughly identical to those of the total spectrum of 1E 0035, which is consistent with the very small colour modulation in the observed orbital light curve (see Sect. 2).

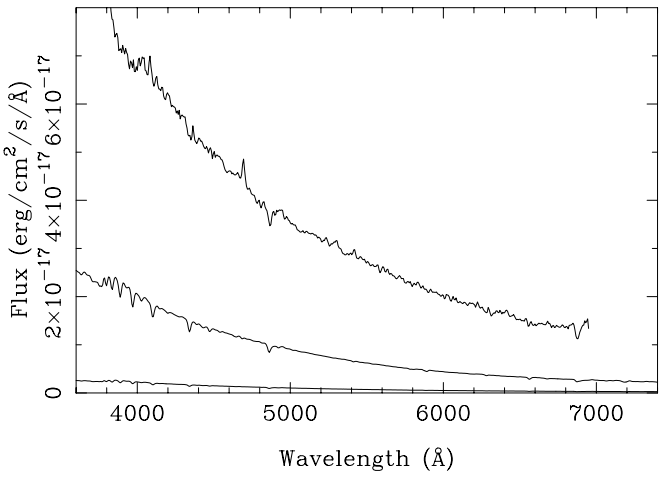

Fig. 10. Average spectrum of 1E 0035 scaled to $V = 20.3$. The lower two spectra are artificial spectra of the irradiated companion star at orbital phases 0 and 0.5, using a composition of observed stellar spectra and the temperature distribution inferred from our light curve modeling ($Q = 2$, $\beta = 5^\circ$, $i = 40^\circ$)

Apparently, the simple approach of summing stellar spectra produces a reasonable estimate of the continuum flux of the irradiated companion star. However, it predicts stronger Hγ and Hδ than observed, while the predicted Hβ is somewhat weaker than observed. Theoretically, we do not expect strong Balmer absorption lines in the spectrum of the heated side of the donor star: as a result of a temperature inversion, soft X-ray irradiation will produce emission cores and may completely fill up the absorption if the irradiation is sufficiently strong. The same holds for Balmer emission from the accretion disk. Stronger X-ray irradiation may explain why C97 observed weaker Balmer absorption lines and Hα in emission.

The fact that the observed Balmer absorption seems to be more prominent at orbital minimum argues against an origin on the companion star or the accretion disk. Instead, it is possible that some of the Balmer absorption (and emission) originates in the strong irradiation-driven stellar wind expected from the companion star and the disk (Van Teeseling & King 1998). This would be consistent with the fact that the absorption is more prominent near optical orbital minimum and that some of the Hβ absorption may trace the orbital motion of the companion star. We conclude that the Balmer lines in 1E 0035 may be a complex mixture of absorption and emission lines from the accretion disk, companion star, and winds from the companion and disk. With a variable irradiation flux and mass loss rate in the winds, the Balmer lines may appear very different on different occasions.

6. Conclusions

1. The U, B, V, and R light curves show an almost perfectly sinusoidal modulation on the 0.171926-day orbital period. We do not find evidence for an asymmetry in the light curve minimum.
2. $B - V$ is significantly variable with a standard deviation of 0.04 mag. This variability shows a weak orbital modulation with an amplitude of 0.03 mag, and with the binary appearing slightly bluer at orbital phase ~ 0.74.
3. Irradiation effects in 1E 0035 are extreme and dominate the optical light curves. The observed modulation is probably completely the result of the changing aspect of the irradiated companion star. The inferred orbital inclination is $\sim 20 - 50^\circ$.
4. Modeling of the light curves suggests $M_1/M_2 < 3$, which is consistent with a supersoft X-ray binary in which the mass transfer is driven by an irradiation-induced wind from the companion star (Van Teeseling & King 1998).
5. Our optical spectra of 1E 0035 show He II$\lambda4686$ in emission and hydrogen Balmer absorption lines, which are variable in strength and in radial velocity. The Balmer lines are probably a complex of different emission and absorption components.
6. The inferred spectrum of the irradiated companion star has a continuum resembling that of a B star, but with significantly weaker Balmer absorption.

Acknowledgements. This research was supported by the DARA under grant 50 OR 96 09 8. We thank Rick Hessman for discussions and comments on the manuscript.

References

Avni Y., 1978, In: Physics and Astrophysics of Neutron Stars and Black Holes, Giacconi R., Ruffini R. (eds.), Amsterdam: North-Holland
Crampton D., Hutchings J.B., Cowley A.P., Schmidtke P.C., 1997, ApJ 489, 903 (C97)
Eggleton P.E., 1983, ApJ 268, 368
Fujimoto M.Y., 1982, ApJ 257, 767
Hessman F.V., Van Teeseling A., Beuermann K., 1997, in: Accretion Phenomena and Related Outflows, IAU Coll. 163, PASP Conf. Ser.
Iben I., 1982, ApJ 259, 244
Jacoby G.H., Hunter D.A., Christian C.A., 1984, ApJS 56, 257
Jordan S., Mürset U., Werner K., 1994, A&A 283, 475
Kahabka P., Ergma E., 1997, A&A 318, 108
Kahabka P., Van den Heuvel E.P.J., 1997, ARA&A 35, 69
Kahabka P., Pietsch W., Hasinger G., 1994, A&A 288, 538
Kopal Z., 1959, Close Binary Systems, New York: Hill & Wiley
Landolt A.U., 1992, AJ 104, 340
Meyer-Hofmeister E., Schandl S., Deufel B., Barwig H., Meyer F., 1998, A&A 331, 612
Ögelman H., Orio M., Krautter J., et al., 1993, Nat. 361, 331
Orio M., Della Valle M., Massone G., Ögelman H., 1994, A&A 289, L11
Parmar A.N, Kahabka P., Hartmann H.W., Heise J., Taylor B.G., 1998, A&A 332, 199
Schandl S., Meyer-Hofmeister E., Meyer F., 1997, A&A 318, 73
Schmidtke P.C., Cowley A.P., McGrath T.K., Hutchings J.B., Crampton D., 1996, AJ 111, 788 (S96)
Seward F.D., Mitchell M., 1981, ApJ 243, 736
Smale A.P., Corbet R.H., Charles P.Q., et al., 1988, MNRAS 233, 51
Stone R.P.S., Baldwin J.A., 1983, MNRAS 204, 347
Van den Heuvel E.P.J., Bhattacharya D., Nomoto K., Rappaport S.A. 1992, A&A 262, 97
Van Teeseling A., 1998, in: Proceedings of the 13th North American Workshop on Cataclysmic Variables, Howell S. et al. (eds.), San Francisco: ASP
Van Teeseling A., King A.R., 1998, A&A, in press

Van Teeseling A., Heise J., Kahabka P., 1996a, in: Compact Stars in Binaries, IAU Symp. 165, Van Paradijs J. et al. (eds.), Kluwer Academic Publishers
Van Teeseling A., Reinsch K., Beuermann K., Thomas H.-C., Pakull M.W., 1996b, in: Supersoft X-ray Sources, Greiner J. (ed.), LNP 472, Springer-Verlag Berlin
Vrtilek S.D., Raymond J.C., Garcia M.R., Verbunt F., Hasinger G., 1990, A&A 235, 162
Westerlund B.E., 1997, The Magellanic Clouds, Cambridge Astrophysics Series 29